Polish Journal of Chemical Technology, 18, 3, 1—9, 10.1515/pjct-2016-0041

Photocatalytic removal of reactive yellow 145 dye from simulated textile wastewaters over supported (Co, Ni)$_3O_4$/Al_2O_3 co-catalyst

Emman J. Mohammad, Abbas J. Lafta*, Salih H. Kahdim

Babylon University, Chemistry Department, College of Science
**Corresponding author: e-mail: abbaslafta2009@ yahoo.com*

The supported co-catalyst (Co, Ni)$_3O_4$/Al_2O_3 was prepared via using a co-precipitation method. Three sets of these materials were prepared by calcination at three different temperatures 500, 600, and 700°C. Crystal structure of the prepared materials was investigated using powder X-rays diffraction (PXRD), Fourier transform infrared spectroscopy (FTIR), Atomic force microscope (AFM), and specific surface area (BET). The activity of the prepared catalysts was investigated by following both of photocatalytic and adsorption removal of Reactive yellow 145 dye (RY 145) from simulated industrial wastewaters. In this study, different reaction conditions were performed such as effect of pH of the reaction mixture, mass dosage of the used catalyst, and effect of temperature. In addition to that adsorption isotherms and reaction kinetics were investigated. Also the activity of these catalysts were investigated after cyclization of the used catalysts.

Keywords: supported co-catalyst, photocatalytic removal of RY 145, removal of RY 145 from wastewaters, Reactive yellow 145, Adsorption processes.

INTRODUCTION

Recently, there was a much interest in the researches that are focused on investigating that are directed toward finding of new methods to remove polluted dyes from industrial wastewaters. Among different types of the being used dyes, azo dyes seem to be most effective type as these dyes are used widely in many textile industries, food, and color paper printing industry[1]. In general, azo dyes have a complex aromatic structure, and they are almost have complex structural azo groups (-N=N-). The deep color of these dyes comes from the presence of the azo groups in such dyes, and hence if these groups are broken then the color can be disappeared. Due to the rigid structure of these compounds, so that it not easy to break these materials into smaller fragments under normal condition.

The presence of these dyes in the effluent industrial wastewaters can produce many types of environmental pollution including air, water, and soil pollution. In addition to that some of these dyes can produce carcinogenic materials and/or releasing some of toxic materials into the ambient environment[2–7]. Generally, tradition ways that can be used to remove dyes from textile industrial wastewaters involve some of physical, biological and chemical methods. Recently, photodegradation methods seem to be interesting alternative method that can be used effectively in removal of these dyes from textile effluents. According to this method, Semiconductors photocatalysts play an important role in dyes removal from their wastewaters[8–11].

Among wide range of the used photocatalysts, alumina (Al_2O_3) seems to be one of the most important supporter materials that can be used as a supporter for many types of conductors and semiconductors photocatalysts. This oxide has large surface area, inert, relatively cheap, thermally stable, easy to prepare, and it easy to cyclized for further usage. Due to all of these excellent properties, it can be used widely in heterogeneous catalyst preparation[12]. Generally, alumina can exist in more than one structural format depending on the calcination temperature, and hence different types of alumina can be produced such as α-Al_2O_3, and γ-Al_2O_3. The first type can be produced upon calcination of aluminum hydroxide at around 1100°C, while the second type can be produced under calcination aluminum hydroxide of around at 400°C[13]. Due to its large surface area and high porosity, it can be used effectively in the removal dyes and others colored compounds from wastewaters and other colored solution. Also it can be used widely as a supporter for others catalytic materials and it can be used in chromatographic methods[13].

Besides alumina, cobalt oxide (Co_3O_4) has important catalytic properties which enable it to be used for many environmental applications. Cobalt oxides have many industrial applications such as colored glasses industries, electrochemical devices[14, 15], and in hydrogenation reactions. Cobalt oxide is an important catalyst that can be used effectively for oxidation of many types of volatile organic compounds. The main drawbacks of this oxide, it may lose some of its activity at high temperatures over than 600°C.

Nickel oxide (Ni_3O_4), also is an important catalytic material that can be used in many industrial and scientific applications such as photochemical reactions, and hydrogenation reactions. Nickel oxide has a distorted structure due to the presences of excess oxygen that make holes between the neighboring ions of Ni^{2+} ions. This leads to oxidation of Ni^{2+} to Ni^{3+}, it's believed that this process is responsible for the oxide color[16]. Generally, the above oxides can be used singly, coupled as well as a supported co-catalyst as a heterogeneous photocatalyst in the heterogeneous photocatalytic systems. One important application of these systems is it use in photocatalytic degradation of environmental pollutants. In this system, photocatalytic degradation is caused breakdown of the molecule into the smaller fragments. The basic principle here is the producing of conduction band electrons and valence band holes upon photoexcitation of the photocatalyst via absorption of light with a proper energy. The produced positive holes react with the electron donor

adsorbed species such as hydroxyl ions on the surface to produce hydroxyl radicals ($OH^{\bullet}$). On the other hand, electrons in the conduction band react with the electron acceptors adsorbed molecules such as O_2 to produce some of reactive species such as $O_2^{\bullet}$, $O^{\bullet -}$ and H_2O_2. These reactive radicals and species are contributed in degradation of polluted materials into volatile organic and inorganic materials such as H_2O and CO_2 and other inorganic materials[17, 18].

The present work, describes study of the photocatalytic removal of reactive yellow 145 dye from the simulated textile industrial wastewaters over synthesized Ni_3O_4_Co_3O_4/Al_2O_3 photocatalyst.

MATERIAL AND METHODS

Material and chemicals

All chemicals that were used in this work were analytical grade and they were used as they provided without any further purification. Aluminum nitrate, $Al(NO_3)_3 \cdot 9H_2O$, Cobalt nitrate hexahydrate $Co(NO_3)_2 \cdot 6H_2O$, nickel nitrate hexahydrate $Ni(NO_3)_2 \cdot 6H_2O$ were obtained from BDH Company with Purity 99.5, 97.9, 99.9% respectively. Sodium carbonate anhydrous Na_2CO_3 obtained from Gmbh with Purity 99.9%, HCl and NaOH were obtained from BDH Company. Reactive yellow 145 it's an azo disperse dye, it has a molecular formula $C_{28}H_{20}ClN_9Na_4O_{16}S_5$ and the molar mass 1026.25 $g \cdot mol^{-1}$ [19] and it was obtained from Hilla Textile Factory.

Catalyst synthesis

The supported co-catalyst was prepared by co-precipitation method, according to this method, 40% of $Co(NO_3)_2 \cdot 6H_2O$, and 40% of $Ni(NO_3)_2 \cdot 6H_2O$ with a ratio of 20% Al $(NO_3) \cdot 9H_2O$ were weighed accurately and dissolved in 400 mL of distilled water with a continuous stirring at room temperature under normal atmospheric conditions. The pH of the resultant mixture was adjusted using a digital pH meter to maintain pH at a required value. To this mixture, Na_2CO_3 (1M) was added drop wisely as a precipitating agent and kept the solution at a temperature around (70–75)°C. Then the value of pH of the produced mixture was kept around (pH = 9). The resultant mixture then was left for (2) hours at same temperature with continuous stirring under air conditions. The obtained mixture filtered of with Buchner filtration flask with a vacuum pump. The obtained solid dried in an oven for overnight at approximately (120)°C. Then this material was calcinated at three different temperatures 500, 600, and 700°C at a heating rate of 10°C/min for 4 hours under normal air atmosphere[20, 21].

CATALYST CHARACTERIZATION

Powder X-ray diffraction (PXRD)

The crystal structure of the prepared co-catalysts was investigated using powder X-ray analysis, Phillips X--ray diffraction with CuKα radiation (1.542 A, 40 KV, 30 MA), in the 2θ range, 10–80 degrees. XRD6000, Shimadzu, Japan.

Fourier transform infrared spectroscopy (FTIR)

Functional groups of the surface of the prepared co-catalysts were investigated using Fourier Transform Infrared Spectroscopy (FTIR), Perkin Elminer Spectrophotometer Company. FTIR spectra were recorded in the range from 400–4000 cm^{-1}, materials were mixed with powder of potassium bromide (KBr) in a ratio of 1:20 prior to run spectrum.

Surface area determination (BET)

The specific surface areas of the prepared co-catalysts were investigated according to BET theory, using prep 060 and Gemini BET machine. According to this technique, 0.05 g of each sample was dried with flushing N_2 gas to remove pre-adsorbed gases in the sample. Then BET specific surface areas of the prepared co-catalysts were performed via adsorption of nitrogen at –196°C.

Atomic force microscopy (AFM)

The prepared co-catalysts were further investigated using atomic force microscopy (AFM) SPM-AA3000 Atomic Force Microscope/ Contact Mode Angstrom Advanced INC., 2005, USA. This device was used to investigate atomic configuration and topography at the surface of the prepared catalysts.

Thermogravimetric analysis (TGA)/DSC

Gravimetric analysis was used to investigate loss in the weight of carbonate catalyst and following a full transition to the corresponding oxides as a function of temperature. In this technique, a certain weight of the prepared carbonate catalyst was taken under an atmosphere condition of % $2O_2$ with rising of temperature to 700°C at a heating rate of 10°C/min.

Photocatalytic activity of the prepared catalyst

Photocatalytic removal of RY145 dye

Photoreaction cell was made up from Pyrex glass with window quartz. This cell has a total volume of 30 mL, irradiation source was lamp- Philips- Holland (250 W) without cover glass as a source of UV radiation. Dye model that was investigated in this study was reactive yellow 145 (RY 145). All experiments were performed by adding the catalyst into the reaction cell which contains (50 ppm, 30 mL) of RY 145 dye solution for each run. The reaction mixture was adjusted to a constant temperature at 23°C. The reaction was initiated by flushing UV radiation after ten minutes of dark reaction. Periodically, 2 mL of reaction samples were withdrawn at each 10 minutes for a period of one hour of reaction duration. These samples were collected and centrifuged carefully to remove any fine particles that may remain with the supernatant liquid. Then the absorbance's were recorded at 418 nm for RY 145 using UV-Visible spectrophotometer (Shimadzu1100A). Photocatalytic removal of the used dye was calculated using the following equation:

%Photodegradation efficiency = $C_0 - C_t / C_0 \times 100$, where C_o, C_t is the initial and the final concentration of RY 145 dye.

Study effect of duration time and catalyst dosages on dye removal

In order to investigate effect of duration time of reaction and the dosage of the used catalyst on the efficiency of dye removal. A series of experiments were performed using 30 mL of 50 ppm of RY145 dye with continuous stirring for one hour using a graduated catalyst masses (0.05, 0.1, 0.15, 0.2 and 0.3 g.). In this study, pH values were adjusted at a desired level using 0.01 M NaOH or 1 M HCl solutions and then the pH values were measured by a pH meter. The absorbance of each sample was measured at λ max = 418. The efficiency of the photocatalytic removal of RY 145 dye was calculated using the relation that was mentioned the above paragraph.

Adsorption ability of the prepared catalyst

Adsorption ability of the prepared catalyst was investigated using an aqueous solution of RY145 dye (50 ppm, 1000 mL). These samples were stirred continuously at room temperature without light with using 0.1 g of the catalyst. The absorbance of the supernatant liquids was recorded at 418 nm.

RESULTS AND DISCUSSION

X-rays diffraction

From the obtained results of XRD patterns for the prepared catalysts, it was found that the crystalline structure was enhanced with elevation of calcination temperature at 500, 600, and 700°C. Besides that, the particle size for these catalysts was increased with increase of calcination temperature. Also form these patterns, it can be seen that there were some deviation in the positions of the peaks and spaces – d for standard values by matching with Joint Committee on Powder Diffraction Standards (JCPDS)[22]. This deviation is acquired by influencing between oxides and XRD patterns of the prepared catalysts as shown in Figure 1.

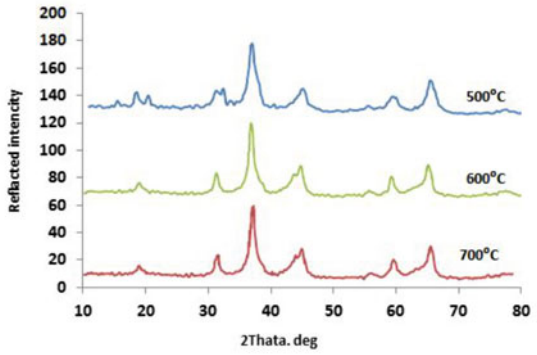

Figure 1. X-ray patterns for the prepared catalyst after calcination at different temperatures 500, 600, 700°C

Fourier Transform Infrared Spectroscopy (FTIR)

FTIR spectra of Ni_3O_4-Co_3O_4/Al_2O_3 showed peak around 569 cm^{-1} which corresponds to cobalt oxide[23], and another peak around 418.55–466.77 cm^{-1} which corresponds to nickel oxide [24]. Also showed a peak at 3431.36 cm^{-1} which corresponds to AlOH. The peak around 1629.85 cm^{-1} is corresponded to γ-Al_2O_3[25]. FTIR spectra for the synthesized catalysts are shown in Figure.2.

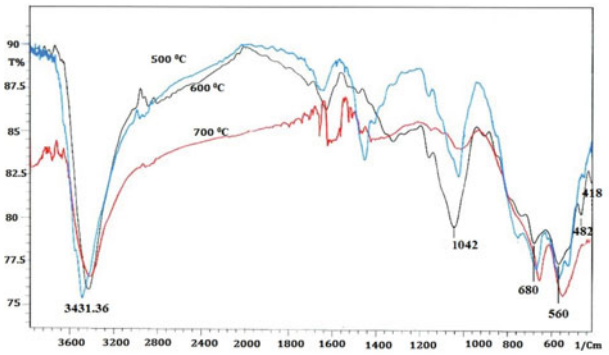

Figure 2. FTIR spectra of the prepared catalyst Ni_3O_4-Co_3O_4/Al_2O_3

Surface area determination (BET)

The results of BET surface areas of the prepared catalysts are shown in Table 1. From these results it was found that the BET surface areas were decreased with increase in calcination temperature. Also there was a decrease in the pore size of the particles under these conditions. This probably due to the effect of sintering processes that occur at high calcination temperatures and this can lead to reduce in BET surface areas of these materials[25–28].

Table 1. BET surface area of the catalyst and pore volume

Calcination temperature, [°C]	BET, [m^2/g]	Pore volume, [cm^3/g]
500	163.235	1.185
600	123.174	1.174
700	95.798	0.255

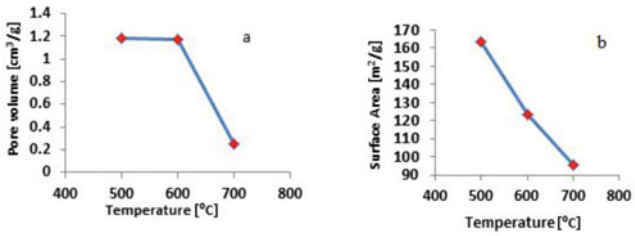

Figure 3. Schematic description of (a) surface area, (b) pore volume of the prepared catalyst

Atomic force microscopy (AFM)

From the obtained images of atomic force microscopy, it can be seen that the average particles diameters of the prepared co-catalysts were decreased with increase in calcination temperature[29]. The average particle size at three calcination temperatures was as follows: at 500°C was 107.87 nm, at 600°C was 107.29 nm, and at 700°C was 105.86 nm. However, this variation in particle size for the prepared catalysts can be attributed to the effect of calcination temperature on the crystal structure of these materials. AFM images of the prepared catalysts are shown in Figure 4.

Thermogravimetric analysis (TGA)/ DSC of the prepared catalysts

Thermal gravimetric analysis technique (TGA) was used to study the changes in losing masses of the prepared catalysts samples at a constant rate of temperature elevation. Figure 5 shows that weight loss 68.1%, 82.9% at 290°C, 700°C respectively from the total weight of

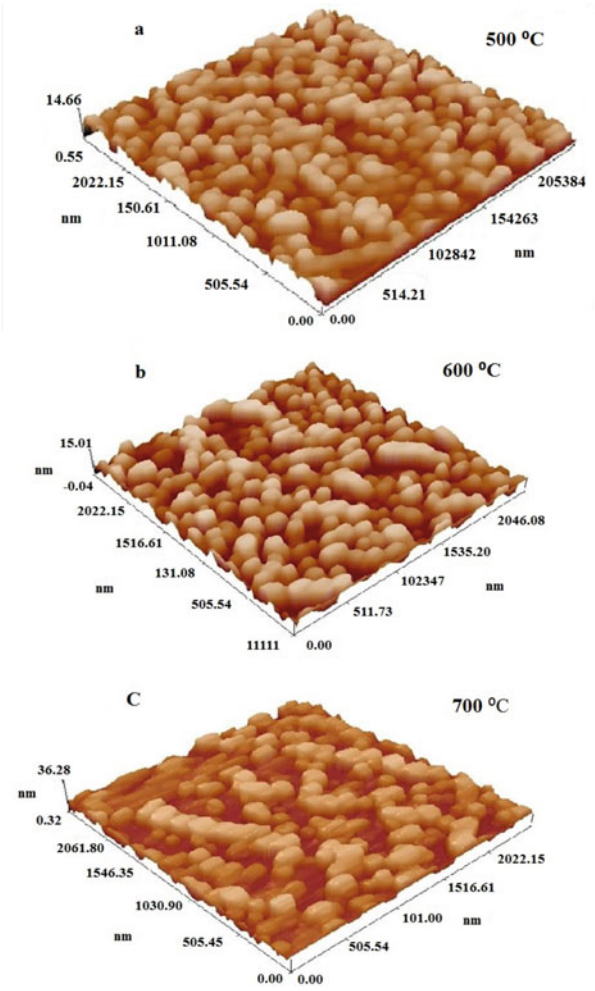

Figure 4. AFM images of Ni_3O_4-Co_3O_4/Al_2O_3 that was calcinated at 500, 600 and 700°C

the catalyst precursor during calcination. Differential scanning calorimeter (DSC) curves showed that upon continuous rise in temperature, the prepared catalytic materials begin to melt and the process is endothermic. At temperatures ranged from 92–100°C water molecules are being lost. The peak at 200–242.5°C is due to lose of CO_2 molecules. The peak at 400–700°C is due to lose of NO_2 and then conversion into the metal oxide [30].

Adsorption Kinetics

Adsorption kinetics was studied using the pseudo-first order, and pseudo-second order the results shows in Figures 6 and 7 and Table 2. The rate constant of adsorption was determined from the pseudo-first order equation as shown below[31]:

$$\ln(q_t - q_e) = \ln(q_e) - k_1 t$$

Where: q_e and q_t (mg/g) are the amounts of the RY 145 adsorbed at equilibrium and at time t (min), respectively, and k_1 (min^{-1}) is the adsorption rate constant.

The pseudo-second order equation based on equilibrium adsorption is expressed in the following equation

$$\frac{t}{q_t} = \frac{1}{k_2 q_e^2} + \frac{t}{q_e}$$

Where: k_2 (g/mg min) is the rate constant of the second order equation.

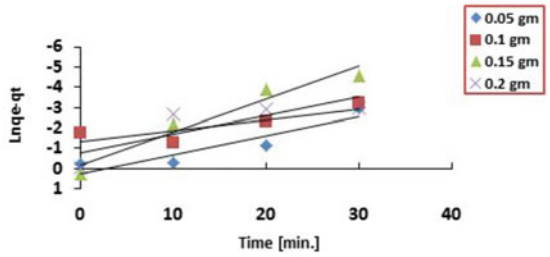

Figure 6. The pseudo-first order kinetic model

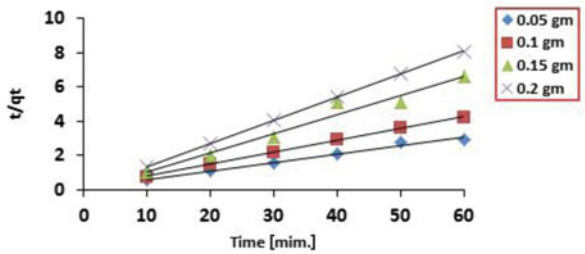

Figure 7. The pseudo-second order kinetic model

Through the results shown in Table 2, it was found that the value of the correction factor for the pseudo second order kinetic model (0.9897–0.9999), higher than

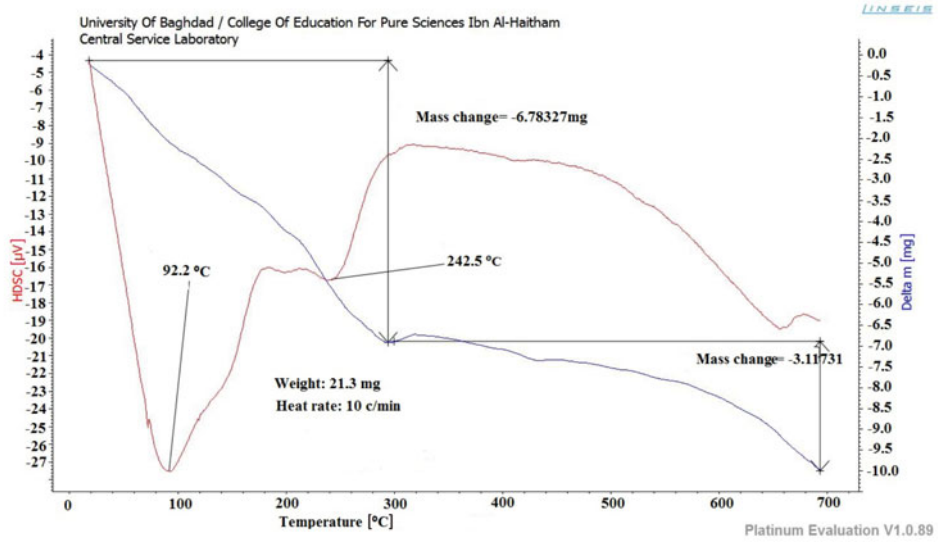

Figure 5. TGA/DSC analysis of the Ni, Co and Al carbonate under 2% O_2

Table 2. The adsorption parameters for RY145 adsorption onto Ni_3O_4-Co_3O_4/Al_2O_3

Wt [g]	Pseudo first order model			
	$q_{e,exp}$ [mg/g]	$q_{e,cal}$ [mg/g]	k_1 [min^{-1}]	R^2
0.05	18.78	1.253	0.0919	0.08401
0.10	13.77	3.768	0.0541	0.7187
0.15	9.77	1.200	0.01623	0.9448
0.20	7.39	2.216	0.0911	0.7058
Wt [g]	Pseudo second order model			
	$q_{e,exp}$ [mg/g]	$q_{e,cal}$ [mg/g]	k_2 [g/mg min]	R^2
0.05	18.78	19.76	0.44	0.9897
0.10	13.77	14.20	0.50	0.9987
0.15	9.77	9.01	1.43	0.9774
0.20	7.39	7.41	4.90	0.9999

the value of the first false correction coefficient. The pseudo-first order kinetic model through the obtained results it is clear that adsorption process of RY 145 dye follows the pseudo-second order kinetic model[32].

Photocatalytic activity of the prepared catalyst

The photocatalytic activity of the prepared catalysts were investigated by following the photocatalytic removal of Reactive yellow 145 that is present in the simulated industrial textile wastewaters over the prepared co-catalysts.

Effect of catalyst dosage on dye removal.

In this part, the effect of catalyst dosage on the phtotocatalytic removal of RY 145 over the prepared co-catalysts was investigated. To investigate that, a series of graduated masses of the co-catalyst were used (0.05, 0.1, 0.15, 0.2 and 0.3 g), with aqueous solution of RY145 dye (30 mL, 50 ppm) under irradiation with UV light at 23°C with continuous stirring under normal atmospheric conditions for a total time of irradiation of one hour. The results of photocatalytic dye removal according to this manner are presented in Figure 8. From these results it can be found that there was an increase in the efficiency of dye removal as the catalyst dose was increased. After a certain value of the catalyst dose (0.1 g), any increase in catalyst dose leads to the reduction in efficiency of dye removal. These observations can be explained according to the laws of photochemistry, initially at low concentrations of catalyst the number of absorbing light particles is few, and therefore there will be a direct proportionality between incident photons and particles of the catalyst. At high concentrations of the catalyst with the same light source intensity, particles of catalyst would form inner filter which absorbs the photons and prevents passing to other side of reaction mixture[33–34]. High doses of the used catalyst can cause light scattering which leads to increase turbidity of the reaction mixture. This point leads to prevent passing of photons of the light into the other parts of reaction mixture due to formation what is called inner filter. From these above observations both low and high doses of the catalyst can give negative results for the photocatalytic processes. So that there is a certain value of the used catalyst that can give best result and in the current study the best catalyst dose was 0.1 gram[35–38].

Effect of pH on photocatalytic removal of RY 145 dye from its aqueous solution

The effect of pH of reaction mixture on t efficiency of photocatalytic removal of RY 145 dye was investigated

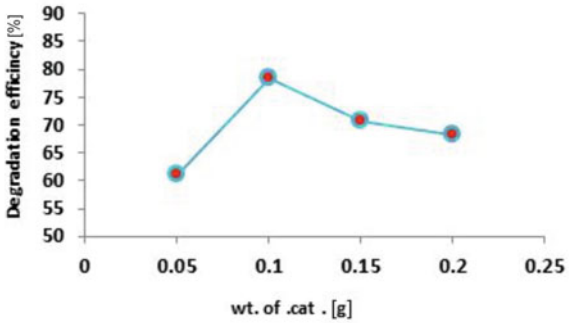

Figure 8. Effect of amount of the used catalyst loading on the efficiency of photocatalytic removal of RY 145 from aqueous solution at (pH = 3, Temp. = 23°C, duration time = 60 min., conc. =50 ppm)

by performing a series of experiments under different pH values with fixation other reaction conditions. The obtained results for photocatalytic dye removal according to these circumstances were highly affected by pH value of the reaction mixture. An important parameter that can effect on photocatalytic activity of Ni_3O_4-Co_3O_4/Al_2O_3 surfaces is the pH of the reaction mixture. The photocatalytic efficiency of dye removal was studied at different pHs values that were ranged from 2 to 8 for reaction mixture. For each case, 0.1 g of catalyst with 30 mL of 50 ppm dye solution at 23°C for 60 minute and under irradiation with UV light was performed. The obtained results are presented in Figure 9. The photocatalytic activity of dye removal was increased with increase in acidity of the reaction mixture and the highest removal efficiency was obtained at pH = 3 and it was around 99.9%. Then any increase in the pH value into alkaline values results in decrease in removal efficiency to 56.1% of RY 145 dye solution. This probably arises from repulsion between the negatively charged surface and the anionic dye molecules[39–41]. Besides that increase in pH values can lead to increase the rate of recombination reaction that occurs between conduction band electrons and valence band holes, this would affect significantly on the efficiency of dye removal from the simulated industrial wastewaters[42–44].

Effect of temperature on photocatalytic removal of RY 145 dye

Effect of temperature on the photocatalytic removal of RY 145 dye was investigated in the range of temperatures 284–296 K with keeping other experimental conditions constant with using 50 ppm in 30 mL of the simulated wastewaters. The used catalyst dose was 0.1 g,

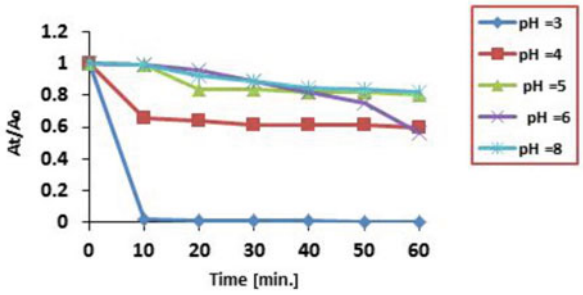

Figure 9. The effect of pH of reaction mixture on photocatalytic removal efficiency of RY 145 at (wt. = 0.1 g., Temp. = 23°C, duration time = 60 min., conc. = 50 ppm)

and the pH value of reaction mixture was kept at (3). The obtained results of photocatalytic dye removal were increased with increase of the reaction temperature to approach 99.9% for the used dye aqueous solution, and the obtained results are summarized in Figure 10. The enhancement in efficiency of dye removal with elevation in reaction temperature can be attributed to effect of temperature on the adsorption/desorption processes. In addition to that, high temperature can lead to increases the rate of formation of free radicals[45, 46]. Generally, in photocatalytic processes reaction temperatures don't effect significantly on the rate of this type of catalyzed reactions as the rate determining step for this reaction is the electron transfer from valence band into the conduction band. It is believed that, increasing in temperature for this type of processes can effect on the amount of adsorption/desorption processes on the surface and these are essential steps for the photocatalytic reactions[47–50].

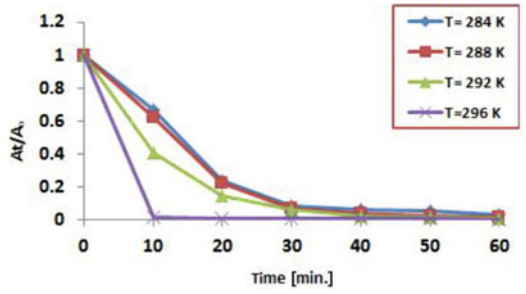

Figure 10. The effect of temperature on the photocatlytic removal efficiency of RY 145 over the prepared co-catalyst at (pH = 3, wt. = 0.1 g., duration time = 60 min., conc. = 50 ppm)

Recycle of the used catalyst

Reuse of the catalyst that was previously used in the removal of RY145 from the simulated wastewater was performed using solvents to wash the catalyst several times, with thermal treatment. The pre-used catalyst was washed with distilled water for several times, then it was dried at 120°C in oven for two hours and heated at 250°C in the furnace for two hours to remove the sticking molecules of dye. The obtained material was used in the removal of RY145 using the same reaction conditions that were used initially and the obtained results are shown in Fig. 11. From these results it was found that the first use catalyst and the second use gave the removal efficiency for this dye 99.9%., and 99.8% respectively. After third time of use, the efficiency of dye removal was decreased to 80.1%. The decrease in the efficiency of dye removal for the re-cyclized catalyst can be attributed to the reduction in the active sites on the surface of the catalyst after one use as well as sticking species that may remain adsorbed on the pores of the catalyst. These observations can lead to reduce the ability of adsorption and consequently reduce its catalytic activity[51–53].

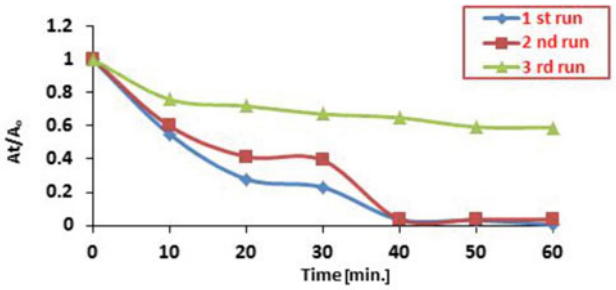

Figure 11. Effect of recycling of the used catalyst on the efficiency of photocatalytic removal of RY145 dye

IR Spectrum of reactive yellow 145 before and after photocatalytic treatment

FTIR spectra for this dye were followed before any treatment (for stock solution of the used dye, 30 ppm). In order to investigate the fate of dye upon photocatalytic treatment its FTIR spectrum was recorded after on hour of the photocatalytic treatment. These spectra are presented in Figure 12 A and B.

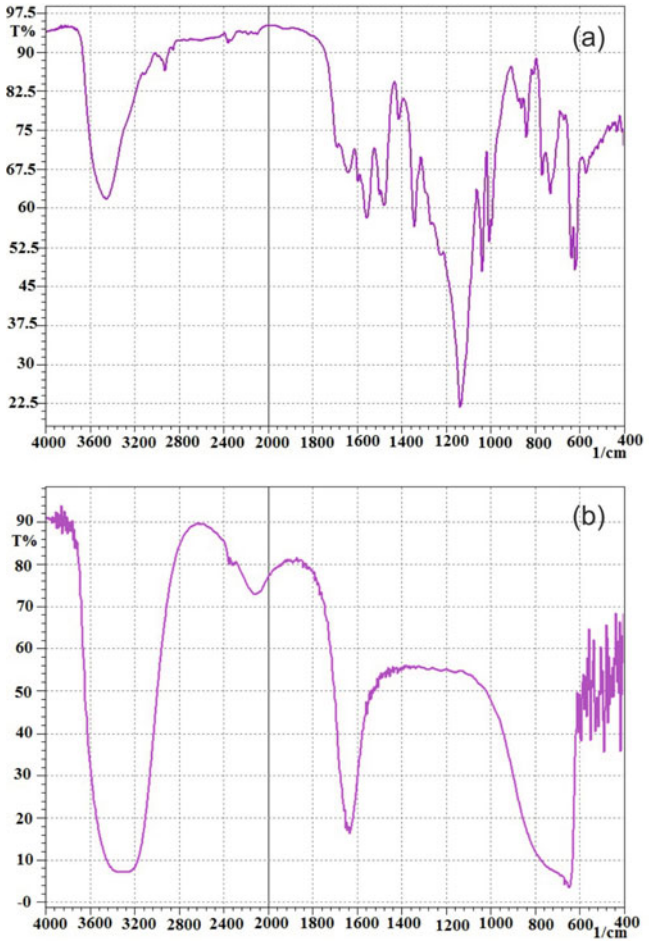

Figure 12. FTIR Spectra for stock solution of RY 145 dye before any treatment (A), and after treatment (B).

FTIR spectrum of stock solution of RY 145 dye is shown in Figure 12 (A). Figure 12 (B) shows FTIR spectrum of dye after 60 minute of treatment with catalyst and UV irradiation. FTIR spectrum of stock solution RY 145 dye before treatment, shows appearance of absorption peak in the fingerprint region 400–800 cm^{-1}. This peak can be assigned to aromatic C = C bond, and C- halogen bond. The peak at 1136.07 cm^{-1} can be assigned to the stretching of C-Cl bond[54]. The appearance of absorption peaks around 1224.8 cm^{-1} can be assigned to stretching of R-SO_3. The peak around 1481.33 cm^{-1} can be assigned to stretching of CH bond, and the peak at 1556.55 cm^{-1} is related to stretching of N = N group[54]. The peak around 1645.28 cm^{-1} is assigned to stretching of C = C aromatic bond, and the peak around 1693.5 cm^{-1} is related to stretching of C = O bond[53]. The peak at 3454.51 cm^{-1} is assigned to stretching of NH acids. The peak around 2800–3000 cm^{-1} can be assigned to stretching of CH-CH aliphatic bond.

When comparing FTIR spectrum of original dye (A) before any treatment with that of after treatment with the used catalyst and irradiation with UV light for 60 minute (B), it can be seen that, the most effective groups were disappeared (B). The broad absorption band at 3200–3500 cm^{-1} is assigned to absorption of OH group, and appearance of peak at 2119.77 cm^{-1} can be assigned to stretching modes of aliphatic C-C bonds. Also appearance of peak around 1637.56 cm^{-1} is assigned to C = C aromatic bond[54]. From these observations it can be concluded that this dye suffers from photocatalytic degradation rather than photocatalytic decolorization.

ACKNOWLEDGMENTS

The authors would like to thank Babylon University, College of Science in Iraq for funding this work as a part of annual research plan for academic staff.

CONCLUSIONS

BET surface areas measurements showed a decrease in the surface area of the prepared materials with increase in calcination temperature. The photocatalytic removal of RY 145 was strongly dependent on the amount of catalyst, pH value, temperature, and illumination time. Also it was found that, complete dye removal was observed when using Ni_3O_4-Co_3O_4/Al_2O_3 under irradiation with UV radiation. From the obtained results in this study, the optimal conditions for degradation of dye under the applied conditions were as follows: pH = 3, catalyst dose 0.1 g/L, temperature = 23°C and illumination time was 60 minute.

LITERATURE CITED

1. Iino, K., Kitano, M., Takeuchi, M., Matsuoka, M. & Anpo M. (2006). Design and development of second generation titration oxide photocatalyst materials operating under visible light irradiation by applying advanced ion-engineering techniques. Current Appl. Physics. 6(6), 982–986. DOI: 10.1016/j.cap.2005.07.002.

2. Tichonovas, M., Krugly, E., Racys, V., Hippler, R., Kauneliene, V., Stasiulaitiene, I. & Martuzevicius D. (2013). Degradation of various textile dyes as wastewater pollutants under dielectric barrier discharge plasma treatment. Chem. Eng. J. 229, 9–19. DOI: 10.1016/j.cej.2013.05.095.

3. Corro, G., Vazquz, O. & Fierro. J. (2005). Strong improvement on CH4 oxidation over Pt/γ-Al_2O_3 catalysts, Catalysis. Communications 6(4), 287–292. DOI: 10.1016/j.catcom.2005.01.012.

4. Cuchillo, O., Lopez, A., Carrillo, L., Hernandez, A., Martinez, L. & Lee S. (2010). Synthesis of TiO_2 using different hydrolysis catalysts and doped with Zn for efficient degradation of aqueous phase pollutants under UV light. Res. Chem.Intermed. 36, 103–113. DOI: 10.1007/s11164-010-0119-4.

5. Song, Y. & Bai, J. (2010). TiO_2–assisted photodegradatoin of Direct Blue 78 in aqueous solution in sunlight. Water Air Soil Pollut. 213(1), 311–317. DOI: 10.1007/s11270-010-0386-0.

6. Wang, S. (2008). A Comparative study of Fenton and Fenton-like reaction kinetics in decolourisation of wastewater. Dyes Pigm. 76(3), 714–720. DOI: 10.1016/j.dyepig.2007.01.012.

7. Khehra, M., Saini, H., Sharma, D., Chadha, B. & Chimni S. (2005). Comparative studies on potential of consortium and constituent pure bacterial isolates to decolorize azo dyes. Water Res. 39(20), 5135–5141. DOI: 10.1016/j.watres.2005.09.033.

8. Robinson, T., McMullan, G., Marchant, R. & Nigam, P. (2001). Remediation of dyes in textile effluent: a critical review on current treatment technologies with a proposed alternative. Bioresource Technology. 77(3), 247–255. DOI: 10.1016/S0960-8524(00)00080-8.

9. Zamora, P., Kunz, A., Moraes, S., Pelegrini, R., Molerio, P., Reyes, J. & Duran, N. (1999). Chemosphere. Degradation of Reactive Dyes I. A Comparative Study of Ozonation, Enzymatic and Photochemical Processes. Chemosphere 38(4), 835–852. DOI: 10.1016/S0045-6535(98)00227-6.

10. Ladakowicz, L., Solecka, M. & Zylla, R. (2001). Biodegradation, decolourisation and detoxification of textile wastewater enhanced by advanced oxidation processes, J. Biotech. 89(2, 3), 175–184. DOI: 10.1016/S0168-1656(01)00296-6.

11. Georgiou, D., Melidis, P., Aivasidis, A. & Gimouhopoulos, K. (2002). Degradation of azo-reacti ve dyes by ultraviolet radiation in the presence of hydrogen peroxide. Dyes Pigm. 52, 69–78. DOI: 10.1016/S0143-7208(01)00078-X.

12. Farrauto, R. & Bartholomew C. (1997). Fundamentals of Industrial Catalytic Processes, Chapman & Hall, Kluwer Academic Publishers, London.

13. Duprez, D., Pereira, P., Barbier, J. & Maurel R. (1980). Catalyst deactivation in toluene steam dealkylation. React. Kin. Catal. Let. 13(3), 217–223. DOI: 10.1007/BF02068569.

14. Pourbaix, M. (1974). Atlas of Electrochemical Equilibrium, Pergamum Press, New York, Translated from French by J.A. Franklin, USA.

15. Pal, J. & Chauhan, P. (2010). Study of physical properties of cobalt oxide (Co_3O_4) nanocrystals. Mater. Character. 61(5), 575–579. DOI: 10.1016/j.matchar.2010.02.017.

16. Sujia, T.T., Hamagamia, T., Kawamurab, T., Yamakia, J. & Masaharu, T. (2005). Laser ablation of cobalt and cobalt oxides in liquids: influence of solvent on composition of prepared nanoparticles. Japan Appl. Surf. Sci. 243(30), 214–219. DOI: 10.1016/j.apsusc.2004.09.065.

17. Hussein, F. (2012). Comparison between Solar and Artificial Photocatalytic Decolorization of Textile Industrial Wastewater. Int. J. Photoener. 2012, 1–10. doi.org/10.1155/2012/793648.

18. Hoffmann, R., Scot Martin, T., Wonyong, C. & Bahnemann, W. (1995). Environmental Applications of Semiconductor Photocatalysis. Chem. Rev. 95(1), 69–96. DOI: 10.1021/cr00033a004.

19. Hussain, B., kashif, D., Ahmad, B., Zubair, A., Yousaf, A., Matloob, I., Muhammad, U., Muhmmmad, Z. & Asim

M. (2013). Degradation Study of C.I Reactive Yellow 145 by Advanced Oxidation Process. Asian J. Chem. 25 (15), 8668–8672. DOI: 10.14233/ajchem.2013.14996.

20. Zofia, L., Narkiewicz, U. & Arabczyk, W. (2013). Cobalt-based Catalysts for Ammonia Decomposition. Materials 6(6), 2400–2409. DOI: 10.3390/ma6062400.

21. Haznan, A., Byoung Sung, A., Chang Soo, K. & Kye Sang, Y. (2007). Preparation and Characterization of MgO−CeO2 Mixed Oxide Catalysts by Modified Coprecipitation Using Ionic Liquids for Dimethyl Carbonate Synthesis. Ind. Engine.Chem. Res. 46(24), 7936–7941. DOI: 10.1021/ie070528d.

22. Sanchai, K. & Hang, H. (2011). Study of NiO -CoO and Co_3O_4 -Ni_3O_4 Solid Solutions in Multiphase Ni -Co -O Systems. Ind. Engine. Chem. Res. 50(4), 2015–2020. DOI: 10.1021/ie101249r.

23. Farhadi, S., Safabakhsh, J. & Zaringhadam, P. (2013). Synthesis, characterization, and investigation of optical and magnetic properties of cobalt oxide (Co3O4) nanoparticles. J. Nanos. Chem. 69(3), 68135–465. DOI: 10.1186/2193-8865-3-69.

24. Ni, Y., Ge, X., Zhang, Z., Liu, H., Zhu, Z. & Ye Q. (2001). A simple reduction-oxidation route to prepare Co 3 O 4 nanocrystals. Mater. Res. Bull. 36(13–14), 2383–2387. DOI: 10.1016/S0025-5408(01)00739-5.

25. Wilson, S. (1979). The dehydration of boehmite, γ-AlOOH, to γ-Al2O3. J. Sol. State Chem. 30(2), 247–255. DOI: 10.1016/0022-4596(79)90106-3.

26. Thirumalairajan, S., Girija, K., Hebalkar,Y., Mangalaraj, D., Viswanathana, C. & Ponpandian, N. (2013). Shape evolution of perovskite LaFeO3 nanostructures: a systematic investigation of growth mechanism properties and morphology dependent photocatalytic activities. RSC Advances 3(20), 7549–7561. DOI: 10.1039/C3RA00006K.

27. Jing, X., Song, S., Wang, J., Ge, L., Jamil, S., Liu, Q., Mann, T., He, Y., Zhang, M., Wei, H. & Liu, L. (2012). Solvothermal synthesis of morphology controllable $CoCO_3$and their conversion to $Co_3O_4$for catalytic application. Pow. Technol. 21, 624–628. DOI: 10.1016/j.powtec.2011.11.040.

28. Wang, G., Cao, D., Yin, C., Gao, Y., Yin, J. & Cheng, L. (2013). Facile synthesis of porous (Co, Mn)3O4 nanowires free-standing on a Ni foam and their catalytic performance for H2O2 electroreduction. J. Mater. Chem. A. 1 (5), 1669–1676. DOI: 10.1039/C2TA00219A.

29. Yamamoto, S., Matsuoka, O., Fukada, I., i Ashida, Y., Honda, T. & Yamamoto, N.(1996). Characterization of pillared montmorillonites with the atomic force microscope (AFM). Journal of Catalysis. 159(2), 401–409. DOI: 10.1006/jcat.1996.0103.

30. Liu Affiliated with Civil and Environmental Engineering School, University of Science and Technology Beijing National Key State Laboratory of Biochemical Engineering, Institute of Process Engineering, Chinese Academy of Sciences, X., Feng, Y. & Li, H. (2011). Preparation of basic magnesium carbonate and its thermal decomposition kinetics in air. J. Cent. South Univ. Technol. 18(6), 1865–1870. DOI: 10.1007/s11771-011-0915-z.

31. Kuśmierek., K.A. & Świątkowski A. (2015). Removal of chlorophenols from aqueous solutions by sorption onto walnut,pistachio and hazelnut shells. Pol. J. Chem. Technol. 17(1), 23–31. DOI: 10.1515/pjct-2015-0005, March 2015.

32. Ferrero, F. (2007). Dye removal by low cost adsorbents: hazelnut shells in comparison with wood sawdust. J. Haz. Mater. 142(1), 144–152. DOI: 10.1016/j.jhazmat.2006.07.072.

33. Monika, S. (2008). Advance oxidation Processes For The Degradation Of Pesticides, Msc Thesis, Department of Biotechnology & Environmental Sciences. Thapar University Patiala, Malaysia.

34. Wang, C., Lee, K., Lyu, D. & Juang, L. (2008). Photocatalytic degradation of C.I. Basic Violet 10 using TiO2 catalysts supported by Y zeolite: an investigation of the effects of operational parameters. Dyes Pigm. 76(3), 817–824. DOI: 10.1016/j.dyepig.2007.02.004.

35. Hussein, F. & Halbus, A. (2012). Rapid Decolorization of Cobalamin. Intern. J. Photoener. 2012, 1–9. DOI: 10.1155/2012/495435.

36. Narendra, T., Oza, A. & Ingale, S. (2014). TiO_2 as an Oxidant for Removal of Chemical Oxygen Demand from Sewage. Univ. J. Environ. Res. Technol. 4(3), 165–171. www.environmentaljournal.org

37. Daneshvar, N., Salari, D. & Khataee, A. (2003). Photocatalytic degradation of azo dye acid red 14 in water: investigation of the effect of operational parameters. J. Photochem. Photobiol. A: Chemistry 157(1), 111–116. DOI: 10.1016/S1010-6030(03)00015-7.

38. Kumar, K., Navjeet, K. & Sukhmehar, S. (2009). Photocatalytic Degradation of Two Commercial Reactive Dyes in Aqueous Phase Using Nanophotocatalysts. Nano. Res. Let. 4(7), 709–716. DOI: 10.1007/s11671-009-9300-3.

39. Daneshvar, N., Aber, S., Seyed Dorraji, M., Khataee, A. & Rasoulifard, M. (2007). Photocatalytic degradation of the insecticide diazinon in the presence of prepared nanocrystalline ZnO powders under irradiation of UV-C light. Separat. Purif. Technol. 58(1), 91–98. DOI:10.1016/j.seppur.2007.07.016.

40. Wang, H., Xie, C., Zhang, W., Cai, S., Yang, Z. & Gui Y. (2007). Comparison of dye degradation efficiency using ZnO powders with various size scales. J. Hazard. Mater. 141(3), 645–652. http://dx.doi.org/10.1155/2012/329082.

41. El-Bahy, Z., Ismail, A. & Mohamed, R. (2009).Enhancement of titania by doping rare earth for photodegradation of organic dye (Direct Blue). Journal of Hazardous Materials. 166(1), 138–143. DOI: 10.1016/j.jhazmat.2008.11.022.

42. Ludwig, C., Byrne, H., Stokke, J., Chadik, P. & Mazyck, M. (2011). Performance of Silica-Titania Carbon Composites for Photocatalytic Degradation of Gray Water. J. Environ.Engine. 137(1), 38–46. DOI.org/10.1061/(ASCE)EE.1943-7870.0000301.

43. Lizama, C., Freer, J., Baeza, J. & Mansilla, H. (2002). Optimized photodegradation of Reactive Blue 19 on TiO2 and ZnO suspensions. Catalysis. Today 76(2), 235–246. DOI: http://dx.doi.org/10.1016/S0920-5861(02)00222-5

44. Movahedi, M., Mahjoub, A. & Janitabar-Darzi, S. (2009). Photodegradation of Congo red in aqueous solution on ZnO as an alternative catalyst to TiO. J. Iranian Chem. Soc. 6(3), 570–577. DOI: 10.1007/BF03246536.

45. Yu Chen, C. (2009). Photocatalytic Degradation of Azo Dye Reactive Orange 16 by TiO2. Water Air Soil Pollut. 202(1), 335–342. DOI: 10.1007/s11270-009-9980-4.

46. Hermann, J. (1999). Heterogeneous Photocatalysis: Fundamentals and Applications to the Removal of Various Types of Aqueous Pollutants. Catal. Today. 53 (1), 115–129. DOI: 10.1016/S0920-5861(99)00107-8.

47. Soares, E., Lansarin, M. & Brazilian, C. (2007). A study of process variablse for the photocatalytic degradation of rahodamine B. Braz. J. Chem. Engine. 24 (1), 29–36. http://www.scielo.br/scielo.php?script=sci_arttext&pid=S0104-66322007000100003

48. Hussein, F., Obies, M. & Drea, A. (2010). Photocatalytic decolorization of bismarck brown R by suspension of titanium dioxide. Inter. J. Chem. Sci. 8(4), 2763–2774. www.sadgurupublications.com/.../2010/89_1176_8(4)2010

49. Attia, A., Kadhim, S. & Hussein, F. (2008). Photocatalytic Degradation of Textile Dyeing Wastewater Using Titanium Dioxide and Zinc Oxide. E-J. Chem. 5(8), 219–223. http://www.e-journals.net

50. Noureddine, B., Samir, Q., Ali, A., Abderrahman, N. & Yhya, A. (2010) Photoctalytic degradation of an azo reactive dye , Reactive yellow84, in water rusing an inindustrilal titanium dioxide coated media. Arabian J. Chem. 3, 279–283.

51. Chakrabarti, S. & Dutta, B. (2004). Photocatalytic degradation of model textile dyes in waste water using ZnO as semiconductor catalyst. J. Hazard. Mater. 112(3), 269–278. DOI: 10.1016/j.jhazmat.2004.05.013.

52. Treybal, R. (1968). Mass Transfer Operations, 2nd ed, McGraw Hill, New York, USA.

53. Al-Khatib, L., Fraige, F., Al-Hwaiti, M. & Al-Khashman, O. (2012). Adsorption from aqueous solution on to natural and acid activated bentonite. Am. J. Environ. Sci. 8(5), 510–522. DOI: 10.3844/ajessp.2012.510.522.

54. Sharma, R., Goyal, K., Chattree, A.R., Baggi, T. & Gupta, A. (2013). Comparative Analysis of Inkjet Printer Inks Extracted from Printed Documents by FT-IR Spectrophotometry. IOSR J. Appl. Chem. 5(3). 36–41. www.iosrjournals.org